

Moment Invariants for 3D Flow Fields via Normalization

Roxana Bujack*
Leipzig University
Germany

Jens Kasten†
Leipzig University
Germany

Ingrid Hotz‡
German Aerospace
Center, Germany

Gerik Scheuermann§
Leipzig University
Germany

Eckhard Hitzer¶
International Christian
University, Japan

ABSTRACT

We generalize the framework of moments and introduce a definition of invariants for three-dimensional vector fields. To do so, we use the method of moment normalization that has been shown to be useful in the two dimensions. Using invariant moments, we show how to search for patterns in these fields independent from their position, orientation and scale. From the first order vector moment tensor, we construct a complete and independent set of descriptors. We test the invariants in queries on synthetic and real world flow fields.

Index Terms: I.4.7 [Image Processing and Computer Vision]: Feature Measurement —Moments; I.5.2 [Pattern Recognition]: Design Methodology —Classifier design and evaluation.

1 INTRODUCTION

Searching for predefined patterns in three dimensional data sets regarding their position, size and principle direction is a hard task, since one has to test every possible translation, scale and rotation of the pattern. In the setting of scalar fields, it has become popular to use *invariant moments* to solve this task. Here, moments are used as a descriptor for the field and the pattern. They can be interpreted as the projection of the data to a certain basis. Based on this concept, moment invariants do not do not change under the aforementioned transformations and therefore they enable a computational affordable comparison of patterns and fields. Since moments have been used for a long time, many different categories of moment invariants have been developed and analyzed [10].

However, the concept is not only applicable to scalar but also to vector data. For two-dimensional vector fields, it has already been demonstrated that moment invariants can be successfully used to search for patterns. Thereby, two different approaches to achieve invariance have been proposed. On the one hand, a set of invariants can be explicitly calculated from the moments [18]. On the other hand, there is the method of normalization [7], which means the pattern is described with respect to an inherent reference size and position [2]. Flusser et al. state that both methods are equivalent [10] for scalar fields. While the first approach is very elegant, it has the disadvantage that it is not very intuitive and hard to generalize to three dimensions. In contrast, the concept of normalization in principle also works for higher dimensions. Here, the major challenge is to find stable reference orientations.

While the analysis of two-dimensional vector fields or flows is still of interest, most applications and real-world simulations are three-dimensional. The visualization and analysis of 3D flows exhibits many new challenges compared to the two-dimensional case. This is also true for the definition and extraction of 3D flow patterns. It concerns the selection and the visualization of patterns but

first of all the mathematical framework to provide invariant descriptors. The goal of this work is to introduce vector moment invariants as basic ingredient for a flow pattern detection framework.

Our novel definition of 3D vector moment invariants makes use of the notion of moment tensors. It has been introduced by Dirilton et al. [7] and further explored by Suk et al. [20] for the definition of 3D moment invariants for scalar fields. The basic idea is to arrange the moments of a given order such that they form a symmetric tensor of this order, exhibiting the typical transformation properties of a tensor. The eigenvectors of the second order moment tensor specify an intrinsic orientation of the pattern, which is used as a reference frame to compare the moments to each other. We follow a similar approach, but there are some fundamental differences from the scalar to the vector case. A similar arrangement of the vector moments leads to an array, which is one order higher than the order of the moments. Still, we can show that the resulting array exhibits the transformation properties of a tensor and justifies the definition of *vector moment tensors*. In contrast to the scalar case, the resulting tensor is not symmetric anymore, which requires a more general approach to define a standard orientation.

The major contribution of this paper can be summarized as:

- Provision of the theoretic framework for the definition of moments for 3D vector fields.
- Derivation of a set of flow field descriptors that are invariant with respect to rotation, background flow, and velocity.
- Experiments using these descriptors for translation, rotation, and scaling invariant pattern recognition of flow fields.

In this paper, we recall the theory of moment tensors for real valued functions and formulate our theory on that basis. Our method is evaluated using a synthetic and two simulated data sets of real-world complexity.

2 RELATED WORK

A complete coverage of all work in the area of vector field visualization goes beyond the scope of this section. Instead, we refer to some overview articles dealing with this topic with different foci: Texture and Feature-Based Flow Visualization [8], Integration-Based Geometric Flow Visualization [14], and Illustrative Flow Visualization [1].

The idea of using moments as pattern descriptors for flow fields has been adopted from the area of image processing and analysis. In 1962, Hu [12] has introduced his famous seven moment invariants to the pattern recognition community. There has been much work since, of which we shortly list the contributions that are most relevant for our work. About one decade after Hu, Dirilton et al. [7] have introduced the notion of moment tensors. The moment tensor contractions to zeroth order are invariant under orthogonal transformations. With this work they laid the foundation for the use of tensor methods to define moment invariants. The first explicit formulation of three 3D moment invariants goes back to Sadjardi et al. [17]. Pinjo et al. [15] estimated the 3D orientation from moment contraction to first order moment tensors. Suk et al. [20] refined the tensor contraction method to zeroth order tensors by giving an algorithm to reduce the number of dependent invariants. An important

*e-mail: bujack@informatik.uni-leipzig.de

†e-mail: kasten@informatik.uni-leipzig.de

‡e-mail: ingrid.hotz@dlr.de

§e-mail: scheuer@informatik.uni-leipzig.de

¶e-mail: hitzer@icu.ac.jp

step further into the direction of the use of moments for 3D pattern recognition was taken by Canterakis [5] who defined the first 3D complete and independent set. He proposed a 3D real function normalization via third grade spherical harmonic moments.

Flusser's work on a complete and independent 2D real moment basis [9] inspired Schlemmer et al. [19, 18] to use moments in the context of flow analysis. For the first time a set of five 2D vector moment invariants was defined. Bujack et al. [2] have generalized the moment normalization method for 2D vector fields. This has led to the first vector invariants, that are complete, independent and flexible to vanishing moments.

In this paper, we combine this normalization approach [2] and the moment tensors [7] to construct moment invariants for 3D vector fields.

3 MOTIVATION: 3D REAL VALUED FUNCTIONS

The method presented in this paper has the following essential features. We will compare functions, by comparing their **moments**. These are the projections of a function to a function space basis. To meaningfully compare the moments of different functions, each function (respectively its moments) is transformed into a predefined standard position. This step is called **normalization**. Once all the functions are in one standard position, their prior position has no influence on their normalized moments. The normalized moments can be used to construct characteristic numbers called **moment invariants**, which do not change under certain transformations.

For the final specification of the technique there are many design options. Especially, the basis functions and the transformations have to be chosen. In this paper we make the two following classical choices. We normalize with respect to translation, rotation, and scaling (TRS). And when it comes to the basis, we use the monomial basis, which has several very useful properties. It is very easy and simple to calculate with and has a clear geometric interpretation. Further, the polynomial space is dense in the space of the continuous functions, which makes its reduction onto a compact volume Ω dense in the space of the square integrable functions $L_2(\Omega)$. Please note that the projection to a basis and the coefficients w.r.t. a basis are only identical if the basis is orthonormal, which the monomial basis is not. Still the two behave equally under the considered transforms.

The method presented in this paper is based on two inspiring sources. On the one hand we use ideas from moment invariants of 2D vector fields [2] and on the other hand from moment invariants of 3D scalar fields [7, 20].

In this section, we recall the latter and summarize the TRS normalization of 3D real valued functions to give a smooth introduction to the method's principles. Later we will generalize it to the normalization for vector fields in a very analogous manner.

3.1 Moments

The moments $m_{p,q,r} \in \mathbb{R}$ are the coefficients of the function with respect to the monomial basis $x^p y^q z^r : \mathbb{R}^3 \rightarrow \mathbb{R}$.

Definition 1. For a three-dimensional function $f : \mathbb{R}^3 \rightarrow \mathbb{R}$ with compact support and $p, q, r \in \mathbb{N}$, the **moment** $m_{p,q,r} \in \mathbb{R}$ of order $p + q + r$ is defined by

$$m_{p,q,r} = \int_{\mathbb{R}^3} x_1^p x_2^q x_3^r f(x) d^3x. \quad (1)$$

On a compact set $\Omega \subset \mathbb{R}^3$, the moments can be interpreted as the projections of the scalar field $f(x)$ onto the basis functions, which are calculated using the $L_2(\Omega)$ scalar product $m_{p,q,r} = \langle x_1^p x_2^q x_3^r, f(x) \rangle_2$.

Example 1. The monomial basis comes along with an intuitive geometric interpretation for its moments. For example, the moment of order zero

$$m_{0,0,0} = \int_{\mathbb{R}^3} f(x) d^3x \quad (2)$$

is simply the mass of an object f . Further, the first order moments form a vector that represents the center of mass via

$$\frac{1}{m_{0,0,0}} \begin{pmatrix} m_{1,0,0} \\ m_{0,1,0} \\ m_{0,0,1} \end{pmatrix}. \quad (3)$$

Dirilton and Newman suggest the use of moment tensors for the construction of moment invariants with respect to orthogonal transforms in [7].

Definition 2. Any form $F_{i_1 \dots i_n j_1 \dots j_m}$ that behaves under an active transformation by the invertible matrix A like

$$F'_{i_1 \dots i_n j_1 \dots j_m} = |\det A|^w \sum_{k_1 \dots k_n} \sum_{l_1 \dots l_m} a_{i_1 k_1} \dots a_{i_n k_n} a_{l_1 j_1}^{-1} \dots a_{l_m j_m}^{-1} F_{k_1 \dots k_n l_1 \dots l_m}. \quad (4)$$

is called a **tensor** of covariant rank m , contravariant rank n , and weight w .

They construct the moment tensors by arranging the moments of each order in a way such that they obey the tensor transformation property (Eq. 4).

Definition 3. For a scalar function $f : \mathbb{R}^3 \rightarrow \mathbb{R}$ with compact support, the **moment tensor** $M_{i_1 \dots i_n}$ of order $n \in \mathbb{N}$ takes the shape

$$M_{i_1 \dots i_n} = \int_{\mathbb{R}^3} x_{i_1} \dots x_{i_n} f(x) d^3x. \quad (5)$$

Thereby, x_{i_j} represents the i_j -th component of $x \in \mathbb{R}^3$, $i_j \in \{1, 2, 3\}$.

This arrangement of the moments of the same order into arrays simplifies the calculation of their behavior under linear transformations, which will be very helpful for the normalization. Cyganski and Orr [6] use moment tensors to determine the orientation of objects. They show that the moment tensor is a contravariant tensor. Now we will refine this statement.

Theorem 1. The moment tensor of order n is a contravariant tensor of rank n and weight 1.

Proof. Let $f'(x) = f(A^{-1}x)$, with $A \in \mathbb{R}^{3 \times 3}$ be an actively linearly transformed version of $f(x)$. Starting out from Definition 3

$$\begin{aligned} M'_{i_1 \dots i_n} &= \int_{\mathbb{R}^3} x_{i_1} \dots x_{i_n} f'(x) d^3x \\ &= \int_{\mathbb{R}^3} x_{i_1} \dots x_{i_n} f(A^{-1}x) d^3x, \end{aligned} \quad (6)$$

we transform the integration variable

$$y = A^{-1}x, \quad x = Ay, \quad \left| \det \frac{\partial x}{\partial y} \right| = |\det A| \quad (7)$$

and get

$$\begin{aligned} M'_{i_1 \dots i_n} &= |\det A| \int_{\mathbb{R}^3} (Ay)_{i_1} \dots (Ay)_{i_n} f(y) d^3y \\ &= |\det A| \int_{\mathbb{R}^3} \sum_{j_1=1}^3 a_{i_1 j_1} y_{j_1} \dots \sum_{j_n=1}^3 a_{i_n j_n} y_{j_n} f(y) d^3y \\ &= |\det A| \sum_{j_1 \dots j_n=1}^3 a_{i_1 j_1} \dots a_{i_n j_n} M_{j_1 \dots j_n}, \end{aligned} \quad (8)$$

which satisfies Definition 2 as a contravariant tensor of rank n and weight 1. \square

3.2 Normalization

We use normalization to construct moment invariants from moments. Normalization is the process of putting a function into a predefined standard position. For real valued functions, we visualize the normalization with respect to translation, rotation, and scaling (TRS) in Figure 1. The transformation of the object itself was only done for demonstration of the principle. In practice, the standard position is achieved just from operations on the moments. That way, no resampling and interpolation of the function is necessary. Once we have determined the parameters that convert a specific function into its standard position, we use Theorem 1 to calculate the normalized moments. For a comprehension of moment invariants, we suggest to look at [10].

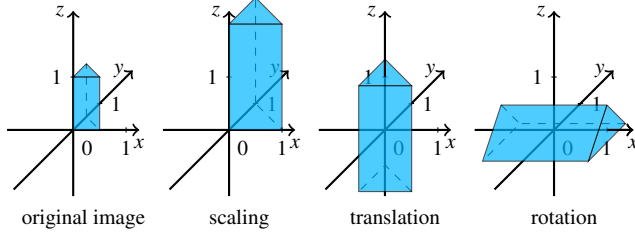


Figure 1: Demonstration of TRS normalization for the example of the 3D characteristic function of a prism.

The generalization of the normalization technique with respect to translation and scaling from 2D to 3D is straight forward. But the structure of rotations is completely different in the two spaces. In 2D, rotations form an Abelian group, whereas in 3D they are no longer commutative. That makes their analysis far more complicated. Therefore, the main part of this section is dedicated to the derivation of normalization with respect to rotation.

3.2.1 Translation

A reasonable choice for a standard position with respect to translation is the claim for the center of mass to coincide with the origin of coordinates, which is the second step in Figure 1. As shown in Example 1, this is equivalent to setting the first order moment tensor to zero, $M_1 = M_2 = M_3 = 0$.

3.2.2 Scaling

Normalization with respect to scaling can be achieved by demanding the function to have a unit mass. This process is the first step in Figure 1. It is equivalent to the claim for the moment of order zero to be one, $M_0 = 1$, compare Example 1.

3.2.3 Rotation

A standard position with respect to rotation can be found using the principal component analysis (PCA). The principal axes of a function are the directions in which it has maximum variance. They are aligned to the coordinate axes, as can be seen in the final step of Figure 1. Even though there are shorter ways in the scalar case, we will show how this normalization can be expressed using the moment tensor because this view on the process allows a rather easy generalization to vector fields and we can reuse the results in the next section. For an introduction to matrix decompositions, we suggest [11].

The second order moment tensor from Definition 3 can be written as an array $\Sigma \in \mathbb{R}^{3 \times 3}$,

$$\Sigma = \begin{pmatrix} M_{11} & M_{12} & M_{13} \\ M_{21} & M_{22} & M_{23} \\ M_{31} & M_{32} & M_{33} \end{pmatrix} \quad (9)$$

We know from Theorem 1 that it is affected by linear transforms via

$$\sigma'_{i_1 i_2} = |\det A| \sum_{j_1, j_2=1}^3 a_{i_1 j_1} a_{i_2 j_2} \sigma_{j_1 j_2}. \quad (10)$$

In principle, this is a standard matrix multiplication

$$\Sigma' = |\det A| \Sigma A^T. \quad (11)$$

We have to be a little careful with this statement. A matrix $S \in \mathbb{R}^{3 \times 3}$ is a tensor of covariant rank one, contravariant rank one and weight zero. Under basis transformations, it behaves like $S' = ASA^{-1}$. The tensor Σ is not a matrix. In order to use standard matrix algebra, we define S as the matrix with the same entries as Σ , i.e. $s_{i_1 i_2} = \sigma_{i_1 i_2}$.

Since S is real valued and symmetric, the spectral theorem guarantees that it can be diagonalized and that its eigenvalues $\lambda_1, \lambda_2, \lambda_3$ and eigenvectors are real valued. Further its eigenvectors form an orthonormal basis. Because they are ambiguous w.r.t. their sign, they form 8 orthogonal matrices $Q_i \in \mathbb{R}^{3 \times 3}, i = 1, \dots, 8$, that satisfy

$$J = \text{diag}(\lambda_1, \lambda_2, \lambda_3) = Q_i S Q_i^{-1} = Q_i S Q_i^T. \quad (12)$$

Obviously, the relation (11) simplifies for orthogonal matrices Q , $\det Q = \pm 1$ to

$$\Sigma' = Q \Sigma Q^T. \quad (13)$$

That means for orthogonal basis transformations, the behavior of the tensor Σ and the matrix S coincide. So it seems reasonable to use the Jordan normal form (JNF) J of S , if we look for a standard position Σ' for Σ . The possible shapes of the JNF for symmetric matrices are explained in detail in the supplementary material.

This alignment along the eigenbasis of the second order moment tensor is equivalent to the alignment along the principal axes of the PCA. It results in the claims for second order moments to satisfy $M_{11} \geq M_{22} \geq M_{33}$ and $M_{12} = M_{13} = M_{23} = 0$. If the eigenvalues coincide, no specified direction can be found. In this case, the brute force approach of comparing the field to the pattern in all possible orientations in the subspace spanned by the corresponding eigenvectors has to be applied.

3.3 Invariant Similarity Measure

For a three-dimensional non vanishing function $f: \mathbb{R}^3 \rightarrow \mathbb{R}$ with compact support Ω , let $f'_i(x) = sf(Q_i^{-1}x) + t$ be a translated, rotated and scaled copy by the parameters $t \in \mathbb{R}^3, s \in \mathbb{R}^+$,

$$s = \frac{1}{M_0}, \quad t = -\frac{1}{M_0} \begin{pmatrix} M_1 \\ M_2 \\ M_3 \end{pmatrix}, \quad (14)$$

and $Q_i \in \mathbb{R}^{3 \times 3}, i = 1, \dots, 8$ each being one of the eight transformation matrices Q satisfying (12). Then, each function f'_i is in the standard position determined by $M_0 = 1, M_1 = M_2 = M_3 = 0, M_{11} \geq M_{22} \geq M_{33}$ and $M_{12} = M_{13} = M_{23} = 0$ and its moments satisfy

$$(M'_i)_{i_1 \dots i_n} = s \sum_{j_1 \dots j_n=1}^3 (q_i^{-1})_{i_1 j_1} \dots (q_i^{-1})_{i_n j_n} M_{j_1 \dots j_n} + t \int_{\Omega} d^3x. \quad (15)$$

If all eigenvalues of the second order moment tensor Σ are different, each set $\{(M'_i)_{i_1 \dots i_m}, m = 0, \dots, n, i = 1, \dots, 8\}$ is TRS invariant.

Considering moments up to order n , the similarity independent from translation, rotation, and scaling of a scalar pattern and a field can therefore be determined from the reciprocal of the Euclidean distance

$$\text{sim} = \left(\sum_{m=0}^n \sum_{i_1 \dots i_m=1}^3 \min_{i=1, \dots, 8} |(M_i^{\text{pat}})_{i_1 \dots i_m} - (M_1^{\text{field}})_{i_1 \dots i_m}|^2 \right)^{-1}. \quad (16)$$

Please note that there is a one to one correspondence of the 8 standard positions of the pattern and the field. That is why comparison of all 8 positions of the pattern to one of the field is sufficient. One of them will match.

4 3D FLOW FIELDS

In this section, we will demonstrate how moment invariants for three-dimensional flow fields can be constructed from normalization of the first order vector moment tensor. The derivation of the technique is very similar to the one for scalar fields from the preceding section, but there are a number of new obstacles to overcome, when we deal with three-dimensional vector fields $v: \mathbb{R}^3 \rightarrow \mathbb{R}^3$

$$v(x) = \begin{pmatrix} v_1(x) \\ v_2(x) \\ v_3(x) \end{pmatrix} = v_1(x)e_1 + v_2(x)e_2 + v_3(x)e_3, \quad (17)$$

with the \mathbb{R}^3 standard basis $\{e_1, e_2, e_3\}$.

4.1 Moments

As in the real valued case, we can construct moments as coefficients of the field $v(x)$ with respect to a function space basis. Again, there are various options for choosing a basis. A direct generalization of the scalar case is the vector monomial basis given by $b_{i_0 i_1 \dots i_n} = e_{i_0} x_{i_1} \dots x_{i_n}$. Since we analyze the 3D vector moments for the first time, we stick with this one because it is very easy to understand and to handle. The first basis vector fields in direction of the x -axis e_1 can be found in Figure 2. The basis is very symmetric. The e_2 and e_3 analogons are rotations of the displayed basis vector fields.

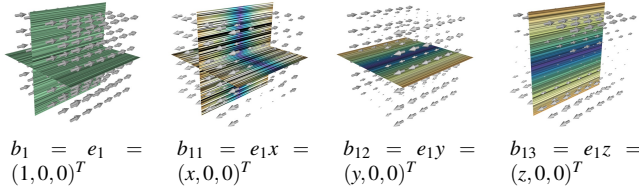


Figure 2: The first basis vector fields visualized with hedgehogs and line integral convolution (LIC) [3]. The color map represents the velocity. Blue means low and red high velocity.

In contrast to the complex basis from the two-dimensional vector field moments in [2], these are not directly the most interesting patterns to flow analysts. But, as can be seen in Figure 3, those can be easily constructed from the basis.

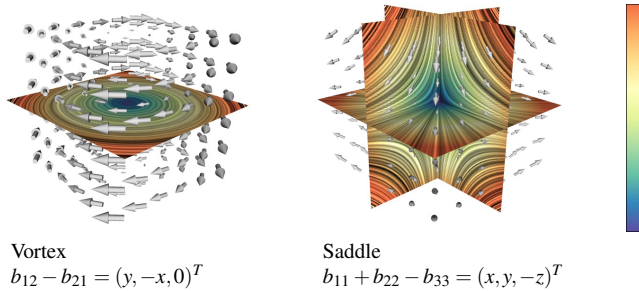


Figure 3: Popular flow patterns can be easily constructed from combinations of the basis vector fields.

Definition 4. For a three-dimensional vector field $v: \mathbb{R}^3 \rightarrow \mathbb{R}^3$ with compact support and $p, q, r \in \mathbb{N}$, the **vector moment** $m_{p,q,r} \in \mathbb{R}^3$ of order $n = p + q + r$ is a vector defined by

$$m_{p,q,r} = \int_{\mathbb{R}^3} x_1^p x_2^q x_3^r v(x) d^3x. \quad (18)$$

Every component of the vector moment consists of the real valued moment of the corresponding component of the vector field. We construct an array that is very similar to the moment tensor of the real valued functions from the previous section. In Theorem 2, we will see that this array is a tensor, too, which justifies the following definition.

Definition 5. For $n \in \mathbb{N}$ and a three-dimensional vector field $v: \mathbb{R}^3 \rightarrow \mathbb{R}^3$ with compact support, the n -th order **vector moment tensor** $M_{i_0 i_1 \dots i_n}$ is defined as

$$M_{i_0 i_1 \dots i_n} = \int_{\mathbb{R}^3} x_{i_1} \dots x_{i_n} v_{i_0}(x) d^3x. \quad (19)$$

Theorem 2. The vector moment tensor of order n is a contravariant tensor of rank $n + 1$ and weight 1.

Proof. Let $A \in \mathbb{R}^{3 \times 3}$ be an invertible matrix and $v'(x) = Av(A^{-1}x): \mathbb{R}^3 \rightarrow \mathbb{R}^3$ an actively transformed version of the vector field $v(x)$, then the vector moment tensor from Definition 5 suffices

$$\begin{aligned} M'_{i_0 i_1 \dots i_n} &= \int_{\mathbb{R}^3} x_{i_1} \dots x_{i_n} (v'(x))_{i_0} d^3x \\ &= \int_{\mathbb{R}^3} x_{i_1} \dots x_{i_n} (Av(A^{-1}x))_{i_0} d^3x \\ &= \int_{\mathbb{R}^3} x_{i_1} \dots x_{i_n} \sum_{j_0=1}^3 a_{i_0 j_0} v_{j_0}(A^{-1}x) d^3x. \end{aligned} \quad (20)$$

If we interchange the sum and the integral, the latter has the same shape as (6). It is the moment tensor of the single real valued component v_{j_0} of the vector field. From the proof of Theorem 1 follows

$$\begin{aligned} M_{i_0 i_1 \dots i_n} &= \sum_{j_0=1}^3 a_{i_0 j_0} |\det A| \sum_{j_1 \dots j_n=1}^3 a_{i_1 j_1} \dots a_{i_n j_n} M_{j_0 j_1 \dots j_n} \\ &= |\det A| \sum_{j_0 \dots j_n=1}^3 a_{i_0 j_0} a_{i_1 j_1} \dots a_{i_n j_n} M_{j_0 j_1 \dots j_n}, \end{aligned} \quad (21)$$

which satisfies Definition 2 as a contravariant tensor of rank $n + 1$ and weight 1. \square

4.2 Normalization

Analogous to the real valued case, we will construct moment invariants for flow fields using normalization.

4.2.1 Considered Transformations

An important difference is the class of transformations that are considered for achieving a standard position, i. e. for invariance. There are many more options to define geometric transformations for vector fields than for scalar functions and other transformations are of significance. For a general vector field, translation, rotation, and scaling can be applied to its argument and its value. That means we generally deal with six central transformations

$$v'(x) = s_o R_o v(s_i R_i x + t_i) + t_o, \quad (22)$$

with the inner and outer scaling factors $s_i, s_o \in \mathbb{R}^+$, translational differences $t_i, t_o \in \mathbb{R}^3$, and rotations $R_i, R_o \in \mathbb{R}^{3 \times 3}$. We illustrate the influence of a rotation applied to a stylized example vector field in the three different ways in Figure 4. Similar effects result from

translation and scaling, too. The inner transformations modify the argument. That means, the location of the vector is changed. The outer transformations modify the value. That means the direction or the velocity of the vector is influenced. The total transformations correspond to a coordinate transformation, where position and value are influenced correspondingly.

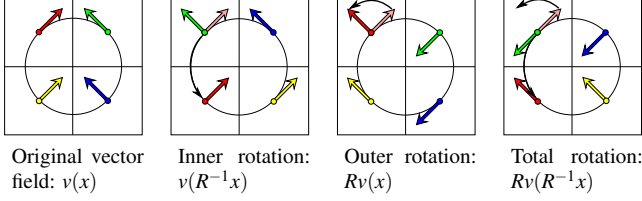


Figure 4: Effect of the rotation operator R_α applied to an example vector field in three different ways.

In the following, we will discuss the six transformations.

Only for the comparison of pattern and field without looking for parts of the field resembling the pattern, considering the **inner translation and scaling** would be reasonable. But because interesting flow patterns usually have a limited spatial extent compared to a whole data set, we do not want to compare fields but only parts of them. This means, we have to restrict the analysis to windows of the size of the pattern. Thus, the inner translation and scaling cannot be covered using moment invariants. Clearly, the moments on one side of the field do not contain information about the other side. This problem is solved by searching at 'all' possible places and for 'all' possible scales in the big vector field. As a result, it is not useful to include these parameters in the calculation (22) we set $t_i = 0, s_i = 1$. Please note that the same situation occurs in the real valued case for a query of a small pattern in a large scalar field.

The **outer translation** can be interpreted as a distortion of the pattern by some background flow or a moving frame of reference. Since we would like to be able to detect moving flow patterns, we will consider normalization with respect to outer translation t_o .

The **outer scale** represents the velocity of the flow. We want to detect the pattern independent from its speed and normalize with respect to outer scaling s_o . Please note that during this operation we will not set every vector to unit length. The ratio between the lengths of the vectors and the velocity pattern are preserved.

The rotation is the most challenging transformation. To be in accordance with rotation of flow fields, we have chosen a spherical window $B \subset \mathbb{R}^3$ for the integration and restrict the transforms to **total rotations**. They influence the orientation of the pattern without changing its inherent structure and satisfy $R_i = R_o^{-1}$.

In Summary, Considered Transformations: All in all, the transformations of a flow field $v(x)$ with respect to which we want to normalize, take the shape

$$v'(x) = sRv(R^{-1}x) + t, \quad (23)$$

with the scaling factor $s \in \mathbb{R}^+$, translational difference $t \in \mathbb{R}^3$, and rotation $R \in \mathbb{R}^{3 \times 3}$. The stepwise normalization of an example flow field is visualized in Figure 5. In the next section, we will show how this special kind of normalization can be produced.

4.2.2 Total Rotation

Finding a standard position with respect to orientation, namely total rotation,

$$v(x)' = Rv(R^{-1}(x)) \quad (24)$$

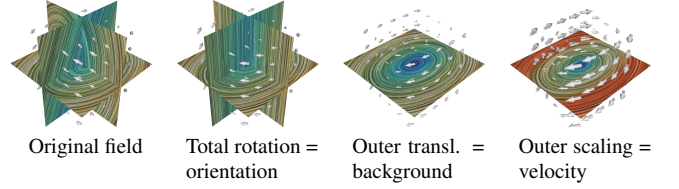


Figure 5: An example flow field is normalized step by step with respect to the considered transformations. The color map represents the velocity. Blue means low and red high velocity.

is the hardest part and will take most of the work. The first order vector moment tensor can be written as the array $\Sigma \in \mathbb{R}^{3 \times 3}$,

$$\Sigma = \begin{pmatrix} M_{11} & M_{12} & M_{13} \\ M_{21} & M_{22} & M_{23} \\ M_{31} & M_{32} & M_{33} \end{pmatrix}. \quad (25)$$

We know from Theorem 2 that it behaves as follows

$$\sigma'_{i_0 i_1} = |\det A| a_{i_0 j_0} a_{i_1 j_1} \sigma_{j_0 j_1} \quad (26)$$

under active transformations by $A \in \mathbb{R}^{3 \times 3}$. Like for the second order moments in the real valued case (11), we can see that this is a weighted matrix multiplication

$$\Sigma' = |\det A| A \Sigma A^T, \quad (27)$$

which implies to proceed analogously. But the situation is a little different. Again let S be the matrix with the same entries as Σ , i. e. $s_{i_0 i_1} = \sigma_{i_0 i_1}$. It is a tensor of covariant rank one, contravariant rank one and weight zero, i. e. it transforms via

$$S' = A S A^{-1}. \quad (28)$$

Can we do everything like in the scalar case now? No. There is a big difference to the real valued case. The tensor Σ , and the matrix S respectively, are not symmetric.

Can we not bring the matrix into JNF? We can bring it into its Jordan normal form by a coordinate transform. But this transform will in general not be orthogonal, i. e.

$$A^T \neq A^{-1}. \quad (29)$$

Even though a matrix would be in Jordan normal form after transformation by A , the contravariant moment tensor

$$\Sigma' = |\det A| A \Sigma A^T \neq A \Sigma A^{-1} = S'. \quad (30)$$

will not. It behaves differently. The behaviors of matrix and tensor only coincide for orthogonal transforms and they will in general not be powerful enough to gain the desired JNF. They can fix only three degrees of freedom, which is enough for symmetric matrices, but not for arbitrary ones. The JNF is too restrictive.

Is there a normal form for orthogonal transformations? Yes. As a solution we can use the Schur form of the matrix [11]. It is an upper triangular matrix

$$U = Q \Sigma Q^T \quad (31)$$

that can be formed by an orthogonal transformation Q . And like in the real valued case, the behavior of our tensor and the matrix coincide for orthogonal transformations. The Schur decomposition can be interpreted as a generalization of the spectral decomposition.

Like the Jordan normal form, it will have the eigenvalues on its diagonal. Only the entries on its upper half will not vanish. In the case of symmetric matrices, the two forms will coincide. In general, the entries on the strict upper triangle are ambiguous.

How can we find an unambiguous normal form? We will make use of the well studied JNF $J = VSV^{-1}$. We calculate the transformation matrix V of the (generalized) eigenvectors in a deterministic way and construct the QR-decomposition of its inverse $V^{-1} = Q^{-1}R^{-1}$. If S has real eigenvalues, J is an upper triangular matrix. From

$$J = VSV^{-1} = RQSQ^{-1}R^{-1} \Leftrightarrow R^{-1}JR = QSQ^{-1} = U, \quad (32)$$

follows that $U = R^{-1}JR$ is upper triangular, too. Because the inverse of an upper triangular matrix as well as the product of upper triangular matrices is an upper triangular matrix. Since U is upper triangular and Q is orthogonal, $U = QSQ^{-1}$ is a Schur decomposition of S . If S has complex eigenvalues, we choose $U = QSQ^{-1}$ as its standard position anyway. It is no triangular matrix in this case, but still unambiguous.

How can we find a deterministic V ? We have seen that even in the real valued case the transformation matrix, which is constructed from the eigenvectors, is not unique. For asymmetric matrices, the situation gets even harder. It is described in Appendix B.

4.2.3 Outer Translation

Additional background flow, namely outer translation,

$$v(x)' = v(x) + t \quad (33)$$

with $t \in \mathbb{R}^3$ influences the vector moment tensor via

$$M'_{i_0 i_1 \dots i_n} = M_{i_0 i_1 \dots i_n} + t_{i_0} \int_B x_{i_1} \dots x_{i_n} d^3x. \quad (34)$$

A reasonable standard is the claim for vanishing background flow, that means vanishing average velocity. Therefore, normalization with respect to outer translation can be done by setting the zeroth order moment tensor to zero. If we solve that for the translation vector $t \in \mathbb{R}^3$, we get

$$M'_{i_0} = 0 \Leftrightarrow t_{i_0} = -\frac{M_{i_0}}{\int_B d^3x}. \quad (35)$$

This operation is generally defined for any non vanishing area $\emptyset \neq B \subset \mathbb{R}^3$. So, we can always preset the moment of order zero to zero to normalize with respect to outer translation.

4.2.4 Outer Scaling

Scaling the velocity

$$v(x)' = sv(x) \quad (36)$$

with $s \in \mathbb{R}^+$ simply influences the moment tensors via

$$M'_{i_0 i_1 \dots i_n} = sM_{i_0 i_1 \dots i_n} \quad (37)$$

Therefore, normalization with respect to scaling can be achieved by demanding a certain non vanishing moment tensor $M_{i_0 i_1 \dots i_n} \neq 0$ to take the value one. If we solve that for the scaling parameter $s \in \mathbb{R}^+$, we get

$$M'_{i_0 i_1 \dots i_n} = 1 \Leftrightarrow s = \frac{1}{M_{i_0 i_1 \dots i_n}}. \quad (38)$$

Other ways of normalization are possible, too. In our algorithm, we choose the first order vector moment tensor in its rotational standard position to have unit Frobenius norm.

4.3 Invariant Similarity Measure

For a three-dimensional flow field $v: \mathbb{R}^3 \rightarrow \mathbb{R}^3$ with spherical compact support B , let

$$v'_i(x) = sQ_i v(Q_i^{-1}x) + t \quad (39)$$

with $i = 1, \dots, 8$ be its outer translated, total rotated and outer scaled copies by the parameters $t \in \mathbb{R}^3, s \in \mathbb{R}^+, Q_i \in \mathbb{R}^{3 \times 3}$. Here each $Q_i \in \mathbb{R}^{3 \times 3}, i = 1, \dots, 8$ is the orthogonal matrix of the QR-decomposition of one of the eight¹ transformation matrices V_i , which transform S into its Jordan normal form J with decreasingly ordered eigenvalues from (32). Further $s = \|J\|_F^{-1} \in \mathbb{R}^+$ is the reciprocal of the Frobenius norm of J and for $i_0 = 1, 2, 3, t \in \mathbb{R}^3$ is determined from

$$t_{i_0} = -\frac{M_{i_0}}{\int_B d^3x}. \quad (40)$$

Then, each function v'_i is in a standard position defined by $M_1 = M_2 = M_3 = 0, M_{11} \geq M_{22} \geq M_{33}, M_{21} = M_{31} = M_{32} = 0$ and $\sum_{i_0, i_1} M_{i_0 i_1}^2 = 1$ and its moments satisfy

$$(M'_i)_{i_0 i_1 \dots i_n} = s \sum_{j_0 \dots j_n=1}^3 (q_i)_{i_0 j_0} (q_i)_{i_1 j_1} \dots (q_i)_{i_n j_n} M_{j_0 j_1 \dots j_n} + t \int_B d^3x. \quad (41)$$

If all eigenvalues of the first order moment tensor Σ are different, each set of moments $\{(M'_i)_{i_1 \dots i_m}, m = 0, \dots, n, i = 1, \dots, 8\}$ is TRS invariant.

Considering moments up to order n , the similarity independent from outer translation, total rotation, and outer scaling of a pattern and a flow field can therefore be determined from

$$sim = \left(\sum_{m=0}^n \sum_{i_0 \dots i_m=1}^3 \min_{i=1, \dots, 8} |(M'_i)^{pat})_{i_0 i_1 \dots i_m} - (M_1^{field})_{i_0 i_1 \dots i_m}|^2 \right)^{-1}. \quad (42)$$

5 RESULTS

In this section, we will present some experiments that are obtained with our method applied to one synthetic data set and two numerical simulations.

First, we designed a synthetic vector field. In a cube $[-4, 4]^3 \subset \mathbb{R}^3$ we place the following flow features:

ID	Position	Basic pattern
	(0,0,0)	very weak source
(A)	(2,-2,2)	sink
(B)	(1,0,2)	oval vortex with core line along the z-axis, drawn out along the x-axis
(C)	(2,2,-2)	bipole in the x-y-plane
(D)	(2,-2,-2)	vortex added to quadrupole in the x-y-plane
(E)	(-2,-2,-2)	saddle
(F)	(-2,2,-2)	vortex with core line along axis $(0, -1, 1)^T$
(G)	(-2,0,2)	long vortex with small diameter and its core line along the y-axis

To get a better impression of the resulting data set, it is illustrated in Figure 6 showing several LIC slices. The weak source in the center is chosen to avoid sections of the vector field to vanish completely to zero, but such that it does not interfere strongly with the other structures. The search pattern is a vortex template, i. e., a simple linear center with a Gaussian dampening as an overlay,

$$v(x) = \begin{pmatrix} y \\ -x \\ 0 \end{pmatrix} e^{-x^2 - y^2 - z^2}. \quad (43)$$

¹As described in the previous section, the sign of each column of V_i is undefined. That leaves us with up to $2^3 = 8$ matrices.

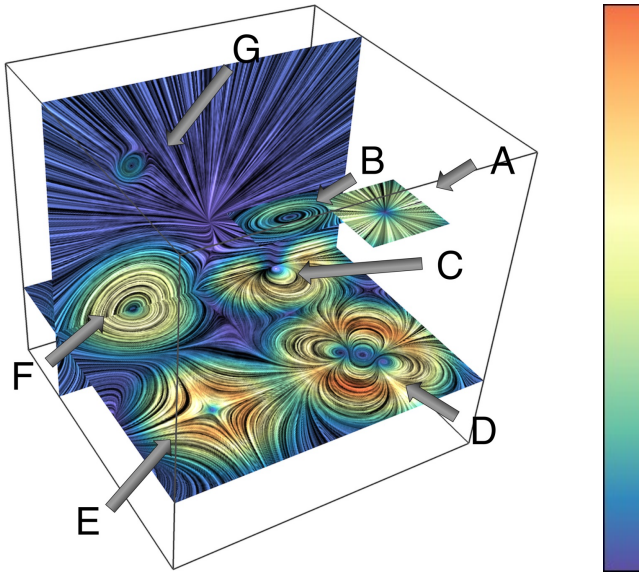


Figure 6: LIC images through the synthetic field. The field contains a sink (A), an oval vortex (B), a bipole (half hidden here) (C), a vortex added to a quadrupole (D), a saddle (E), a short vortex (F), and a long vortex (G).

The similarity is measured as described in 4.3. For each grid point and each scale, we test if its similarity is higher than most of its neighbors. Then, we render a sphere with the following properties: (a) the position of the match is the center of the sphere, (b) the scale of the pattern is the radius of the sphere, and (c) the similarity to the vortex defines the density of the sphere. Whenever two spheres intersect, the higher density value is stored. More detail and the algorithm in pseudo-code can be found in the supplementary material.

The result is a three-dimensional real valued function, which is visualized using volume rendering in Figure 7 (a) with the transfer function from Figure 7 (b). The moments are computed up to second grade.

The volume rendering is supported by a selection of illuminated streamlines in Figure 7. The seeding of the streamlines is driven by the similarity of the pattern with the field. The higher the similarity, the higher the probability of a point to be a seed point of a streamline. This technique is a representative example for all kinds of visualization methods, that may cover up important parts of the flow field if applied to the the whole 3D data set. Using our similarity field as region of interest (ROI), many well known algorithms can be steered directly to only work at the positions where the field is of interest to the flow field analysts and therefore avoid clutter.

In the volume rendering in Figure 7, the following observations can be made: (a) all vortex-like structures are detected with a high and clearly visible similarity value, (b) the size of the spheres indicate the size of the patterns as expected, (c) for larger elongated structures, neighboring spheres combine to large oval ellipsoids, giving insight into the extent and alignment of the structure, and (d) the similarity value is smaller for the distorted vortices: the oval one, the bipole and the quadrupole.

The delta wing is the second data set in our evaluation. The data set results from a simulation of air flow around a single delta wing configuration at subsonic speed and was computed in the context of numerical research into vortex breakdown [16]. The initial high angle of attack increases over time. Although the simulation con-

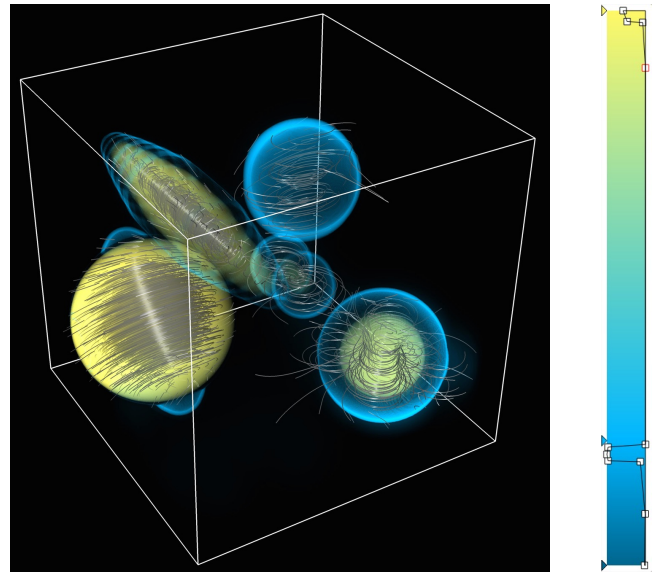


Figure 7: (a) Left: Volume rendering of the spheres field. The streamlines are seeded by similarity of the moments. (b) Right: The transfer function for the volume rendering.

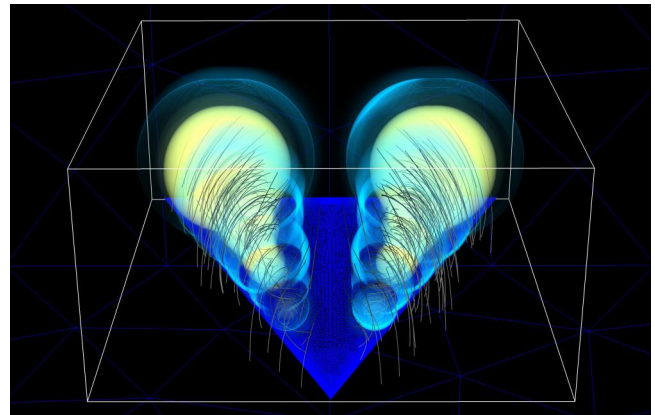


Figure 8: Volume rendering of the similarity field of the delta wing data set using a vortex template.

tains multiple time steps, we limit our analysis to a single time step in this paper that contains 11,915,131 tetrahedron and prism cells. We further cut out the area directly above the delta wing. Analogously to the first data set, we used a vortex as search pattern.

The visualization in Figure 8 is chosen analogous to the other data sets. The two tip vortices that are well known for the delta wing are well extracted. Due to the spatial extent of the moments, it can also be seen very nicely how the vortices grow as they flow along the delta wing. A nice observation can be made at the streamlines, which again have been seeded with probability correlated to the similarity. They underline the vortex structures that have been found. Because of the high velocity of the delta wing, the main direction of the air is towards its rear. Therefore, the vortices are distorted to elongated swirls. The moment invariants are not affected by this. Because of their invariance with respect to background flow, they fully recognize the vortices.

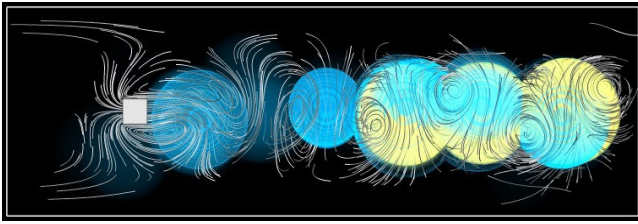


Figure 9: The similarity of the von-Kármán street to the double vortex on its very right under orthographic projection.

The third data set is a numerical simulation of a flow behind a square cylinder with $Re = 200$, resulting in a 3D version of the well known von-Kármán vortex street. The data is a direct numerical Navier Stokes simulation by Camarri et al. [4] which is publicly available [13]. We use a uniformly resampled version which has been provided by Weinkauff and is also used in von Funck et al. [21]. As search pattern we have selected an example pattern from the data set, the last vortex pair corresponding to the yellow sphere on the very right in Fig. 9. This choice shows that our method is not restricted to analytical pattern definitions.

The result can be seen in Fig. 9 using a visualization analogously to the other data sets. It shows the volume rendering and the importance of streamline seeding for the similarity field. For the streamline visualization we subtracted the medium flow from the data. Please note that the pattern search has been performed on the original data set with its natural background flow. The algorithm detects the repetitions of the double vortex pattern along the vortex street very well. It can also be observed that the similarity becomes stronger the nearer the vortices are to the example-pattern we searched for.

6 CONCLUSIONS

With this paper, we have laid the theoretical foundation for the use of vector moment invariants for the analysis of 3D flow fields with respect to interesting patterns. The major contribution is the generalization of the normalization approach from scalar fields to vector fields. Due to the fact that the resulting vector moment tensor is not symmetric as in the scalar case, conceptual changes were necessary and a solution to this problem has been presented. Further, we have performed first experiments using a set of vector moment invariants searching for patterns in one analytically defined vector field and two data sets resulting from a numerical simulation. In all cases, the moments behave as expected.

Still many more steps have to be done in order to come to an easy to use framework based on vector moment invariants. Open issues that need a closer inspection in the future include the artifacts due to the discrete sampling of the field for the moment computation. We further want to explore more visualization options. Especially scalar field topology seems to provide an interesting concept for the investigation of the similarity field. Also the development of an interface for an easy design of new query patterns is envisioned. But in summary, we are convinced that the proposed moments are a powerful tool for flow field exploration.

ACKNOWLEDGMENTS

We would like to thank the FAnToM development group from Leipzig University for providing the environment for the visualization of the presented work, especially Steven Schlegel and Stefan Koch. This work was partially supported by the European Social Fund (Application No. 100098251).

REFERENCES

- [1] A. Brambilla, R. Carnecky, R. Peikert, I. Viola, and H. Hauser. Illustrative Flow Visualization: State of the Art, Trends and Challenges. *EG 2012, State of the Art Reports*:75–94, 2012.
- [2] R. Bujack, I. Hotz, G. Scheuermann, and E. Hitzler. Moment Invariants for 2D Flow Fields via Normalization. In *Proceedings of the 2014 IEEE Pacific Visualization Symposium, PacificVis 2014 in Yokohama, Japan*, 2014.
- [3] B. Cabral and L. C. Leedom. Imaging vector fields using line integral convolution. In *Proceedings of the 20th annual conference on Computer graphics and interactive techniques, SIGGRAPH '93*, pages 263–270. ACM, 1993.
- [4] S. Camarri, M.-V. Salvetti, M. Buffoni, and A. Iollo. Simulation of the three-dimensional flow around a square cylinder between parallel walls at moderate Reynolds numbers. In *XVII Congresso di Meccanica Teorica ed Applicata*, 2005.
- [5] N. Canterakis. Complete moment invariants and pose determination for orthogonal transformations of 3D objects. In *Mustererkennung 1996, 18. DAGM Symposium, Informatik aktuell*, pages 339–350. Springer, 1996.
- [6] D. Cyganski and J. A. Orr. Applications of tensor theory to object recognition and orientation determination. *Pattern Analysis and Machine Intelligence, IEEE Transactions on*, PAMI-7(6):662–673, 1985.
- [7] H. Dirilten and T. Newman. Pattern matching under affine transformations. *IEEE Transactions on Computers*, 26(3):314–317, 1977.
- [8] G. Erlebacher, C. Garth, R. S. Laramée, H. Theisel, X. Tricoche, T. Weinkauff, and D. Weiskopf. Texture and feature-based flow visualization - methodology and application. In *IEEE Visualization Tutorial*, 2006.
- [9] J. Flusser. On the independence of rotation moment invariants. *Pattern Recognition*, 33(9):1405–1410, 2000.
- [10] J. Flusser, B. Zitova, and T. Suk. *Moments and Moment Invariants in Pattern Recognition*. Wiley, 2009.
- [11] R. A. Horn and C. R. Johnson. *Matrix Analysis*. Cambridge University Press, 1990.
- [12] M.-K. Hu. Visual pattern recognition by moment invariants. *IRE Transactions on Information Theory*, 8(2):179–187, 1962.
- [13] International CFD Database, <http://cfd.cineca.it/>.
- [14] T. McLoughlin, R. S. Laramée, R. Peikert, F. H. Post, and M. Chen. Over Two Decades of Integration-Based, Geometric Flow Visualization. In *EG 2009 - State of the Art Reports*, pages 73–92, 2009.
- [15] Z. Pinjo, D. Cyganski, and J. A. Orr. Determination of 3-d object orientation from projections. *Pattern Recognition Letters*, 3(5):351–356, 1985.
- [16] M. Rütten. *Topologische Untersuchung des Wirbelplatzens zur Identifikation von Wirbelplatzparametern*. PhD thesis, Helmut-Schmidt-Universität Hamburg, 2005.
- [17] F. A. Sadjadi and E. L. Hall. Three-dimensional moment invariants. *Pattern Analysis and Machine Intelligence, IEEE Transactions on*, PAMI-2(2):127–136, 1980.
- [18] M. Schlemmer, M. Heringer, F. Morr, I. Hotz, M. Hering-Bertram, C. Garth, W. Kollmann, B. Hamann, and H. Hagen. Moment Invariants for the Analysis of 2D Flow Fields. *IEEE Transactions on Visualization and Computer Graphics*, 13(6):1743–1750, 2007.
- [19] M. Schlemmer, I. Hotz, B. Hamann, and H. Hagen. Comparative visualization of two-dimensional flow data using moment invariants. In *Proceedings of Vision, Modeling, and Visualization (VMV'09)*, volume 1, pages 255–264, 2009.
- [20] T. Suk and J. Flusser. Tensor method for constructing 3d moment invariants. In *Computer Analysis of Images and Patterns*, volume 6855 of *Lecture Notes in Computer Science*, pages 212–219. Springer Berlin, Heidelberg, 2011.
- [21] W. von Funck, T. Weinkauff, H. Theisel, and H.-P. Seidel. Smoke surfaces: An interactive flow visualization technique inspired by real-world flow experiments. *IEEE Transactions on Visualization and Computer Graphics (Proceedings Visualization 2008)*, 14(6):1396–1403, November - December 2008.